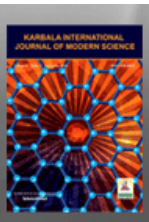

Karbala International Journal of Modern Science

Volume 8 | Issue 3 Article 21

Studying The Physical and Biological Characteristics of Denture Base Resin PMMA Reinforced With ZrO2 and TiO2 Nanoparticles

Fatin A. Asim
Applied Science Department, University of Technology, as.18.17@grad.uotechnology.edu.iq

Entessar H.A. Al-Mosaweb
Applied Science Department, University of Technology

Wafaa A. Hussain
Applied Science Department, University of Technology

Recommended Citation

Asim, Fatin A.; Al-Mosaweb, Entessar H.A.; and Hussain, Wafaa A. (2022) "Studying The Physical and Biological Characteristics of Denture Base Resin PMMA Reinforced With ZrO2 and TiO2 Nanoparticles," *Karbala International Journal of Modern Science*: Vol. 8 : Iss. 3 , Article 21.
Available at: https://doi.org/10.33640/2405-609X.3251

Studying The Physical and Biological Characteristics of Denture Base Resin PMMA Reinforced With ZrO2 and TiO2 Nanoparticles

Abstract

Polymethyl methacrylate (PMMA) suffers from poor mechanical properties that limit its application in the bio-medical field. In this study, PMMA was reinforced with zirconium dioxide (ZrO2) and titanium dioxide (TiO2) nanopar-ticles; subsequently, the hardness, porosity, biocompatibility, bacterial adhesion, and colonization of the reinforced PMMA with various oxide nanoparticles were characterized. The results of this study indicated that reinforced material inhibits bacterial growth and decreases bacterial adhesion by decreasing porosity and increasing PMMA hardness. Based on the findings, 3 wt% PMMA-ZrO2 and 3 wt% PMMA-ZrO2 -TiO2 composites significantly inhibited bacterial growth and adherence while maintaining hemolysis PT and INR and enhancing the hardness and decreasing porosity.

Keywords

PMMA; TiO2; ZrO2; Hemolysis; Bacterial adhesion

RESEARCH PAPER

Studying the Physical and Biological Characteristics of Denture Base Resin PMMA Reinforced With ZrO_2 and TiO_2 Nanoparticles

Fatin Assim Youssif*, Entessar H.A. Al-Mosawe, Wafaa A. Hussain

Applied Science Department, University of Technology, Baghdad, Iraq

Abstract

Polymethyl methacrylate (PMMA) suffers from poor mechanical properties that limit its application in the biomedical field. In this study, PMMA was reinforced with zirconium dioxide (ZrO_2) and titanium dioxide (TiO_2) nanoparticles; subsequently, the hardness, porosity, biocompatibility, bacterial adhesion, and colonization of the reinforced PMMA with various oxide nanoparticles were characterized. The results of this study indicated that reinforced material inhibits bacterial growth and decreases bacterial adhesion by decreasing porosity and increasing PMMA hardness. Based on the findings, 3 wt% PMMA-ZrO_2 and 3 wt% PMMA-ZrO_2 -TiO_2 composites significantly inhibited bacterial growth and adherence while maintaining hemolysis PT and INR and enhancing the hardness and decreasing porosity.

Keywords: PMMA, TiO_2, ZrO_2, Hemolysis, Bacterial adhesion

1. Introduction

In recent years, biomaterial fields have become an exciting area for many researchers in different domains [1]. Polymethyl methacrylate (PMMA) is the most common material that is used in dentures for many reasons, such as color-matching, ease of processing, stability in the oral environment, low cost, nontoxic, and tasteless [2,3]. Despite this, some disadvantages need to be solved, for example, the adhesion and colonization of certain microorganisms on PMMA dentures caused by the surface roughness and porosity of the PMMA [4,5], which lead to plaque organization or other oral diseases [6], such as candidiasis, dental caries, gum disease, and even pneumonia [7,8].

Nanomaterials have become the main limelight of many researchers in different medical fields [9–13], designing anti-microorganism drugs via nanoparticles strategies using their physicochemical properties, like, as ultra-small shapes, increased chemical reactivity, and high surface-area-to-mass ratios. Nanoparticles (NPs) may be a potential treatment and prevention method for dental infections [14].

Reinforced acrylic dentures by NPs can decrease the porosity of PMMA due to the low porosity of nanocomposites [15] and reduce the roughness by using polishing techniques that can reduce the ability of microbial adhesion [16].

Metal and metal oxide NPs such as zinc oxide, zirconium oxide, gold, silver, and titanium oxide nanoparticles have received attention due to their antibacterial properties against harmful microbes. They are very tiny and possess several sophisticated physical and chemical properties. They have been employed as antibacterial agents because of their advanced properties. Due to their tiny size, such nanoparticles may easily infiltrate microbial cells and trigger inhibitory processes inside them. The bacteriostatic or bactericidal impact of nanoparticles is achieved through either restricting their food source or destroying their cell membrane [17]. Sundrarajan et al. [18] discovered that the

Received 29 March 2022; revised 13 June 2022; accepted 16 June 2022.
Available online 1 August 2022

* Corresponding author at:
E-mail addresses: as.18.17@grad.uotechnology.edu.iq (F.A. Youssif), entesar_mosawi@yahoo.com (E.H.A. Al-Mosawe), 100067@uotechnology.edu.iq (W.A. Hussain).

https://doi.org/10.33640/2405-609X.3251

investigated ZrO_2 NPs have antibacterial and antifungal properties. Furthermore, Ahmed A. Thamir et al. demonstrated the antibacterial efficacy of ZrO_2 NPs synthesized using the sol–gel process against pathogenic bacteria such as *Escherichia coli (E. coli)* and *Staphylococcus aureus (S. aureus)* [19].

We utilized titanium dioxide nanoparticles (TiO_2-NPs) in this investigation for various reasons, including their cheap cost, chemical inertness, nontoxicity, high hardness, corrosion resistance, and antibacterial activity [20].

Zirconium dioxide nanoparticles (ZrO_2-NPs) are an essential substance in industrial and advanced biomaterials, and they have also been employed in this study due to their unique qualities, which include chemical resistance and remarkable mechanical strength [21,22]. Its outstanding biocompatibility is matched by its low cytotoxicity, excellent carry properties of ZrO_2-NPs, and good corrosion resistance, metallic characteristics, and hue, which are similar to those of a tooth. Therefore, ZrO_2 is widely utilized in dental implants as a common biomaterial [23].

Due to the photocatalytic characteristics of TiO_2 NPs and ZrO_2 NPs [24], microorganisms are decomposed due to the generation of reactive oxygen species (ROS) such as O_2, OH, H_2O_2, and HO_2. ROS interacts with cell membranes, Deoxyribonucleic acid (DNA), and thiol groups in proteins to have antimicrobial effects. Certain classical bactericidal medicines and nanomaterials produce ROS as an alternate or primary antibacterial action. These ROS act as both therapeutic and toxic chemicals [25]; they are often used to treat or prevent soft tissue infections, but not systemic infections [26]. In addition, the attachment of TiO_2 NPs to the cell membranes of many species may impact and disrupt the permeability of the cells, generate oxidative stressors, and impede cell proliferation [19,27–29].

However, (Verran et al.) [30] indicated that the intrinsic propensity of nanoparticles to generate radicals might affect their antibacterial characteristics.

In this study, we used different ratios of TiO_2-NPs and ZrO_2-NPs (1 wt%, 2 wt%, 3 wt%, and 10 wt%) also 3 wt% as a mix between TiO_2-NPs and ZrO_2-NPs to prepare the PMMA-NPs composite samples, to study the inhibitory effect of the oxide nanoparticle composites on microbial adhesion and colonization, reduce the porosity that might decrease the bacterial adhesion on the denture, determine the impact of nanoparticle composites on hardness, and human blood biocompatibility (hemolysis, PT, and INR).

2. Materials and methods

2.1. Materials and reagents

Crystal violet dye (BDH, England), Lishman stain (Sigma, USA), Ethylenediaminetetraacetic acid (EDTA) (US Biological, US), yellow stone (ISO 6873, Firenze-Italy), normal saline solution (Rasan Pharmaceutical, Iraq), prothrombin time (PT) (human, Germany), international normalized ratio (INR) (human, Germany), phosphate buffer saline components (BDH, England), Heat-polymerized resin PMMA (Superacryl Plus powder, SpofaDental a.s., Jicin, Czech Republic), methyl methacrylate (MMA) (Respal NF: Heat Curing Resin (Liquid) Spd, Dentaltix, Madrid, Spain), and sodium citrate tubes (biozek medical, Netherlands), MacConkey agar (Oxoid, England), nutrient agar (Oxoid, England), TiO_2-NPs (hongwu international group Ltd, China), The remaining chemicals were used at analytical concentrations.

2.2. Preparation of ZrO_2 nanoparticles

The typical procedure for preparing ZrO_2 nanoparticles ($ZrOC_{l2}.8H_2O$) was mixed with deionized water, and NaOH then has applied dropwise mixture until the pH reached 7, as well as the white slurry was formed and precipitated, then retained in an air oven at 90 °C for 2 hrs and then 400 °C for 1 hrs, using a previously developed procedure [31]. After sintering, the resulting powder was crushed until given a fine powder, as shown in Fig. 1.

2.3. ZrO_2 nanoparticles characterization

2.3.1. X- Ray Diffraction technique (XRD)

X-Ray Diffraction)XRD(was chosen to study the crystal structure of ZrO_2 nanoparticles; the device generated Cu-k radiation with a wavelength of (= 0.154 nm) at 40 mA and 40 kV.

The samples were scanned while still at room temperature. Day Petronic Company in Tehran, Iran, carried out this analysis.

2.3.2. Energy-dispersive X-ray spectroscopy (EDX) and scanning electron microscope (SEM)

Scanning electron microscope (SEM) is a sort of high-resolution electron microscopy in which a powerful electron beam is used to probe a specimen on a very tiny scale in order to get further details about nanoparticles. These micro and nanosized materials may be monitored in real-time using this surface imaging technology to monitor their production, size, distribution, and shape.

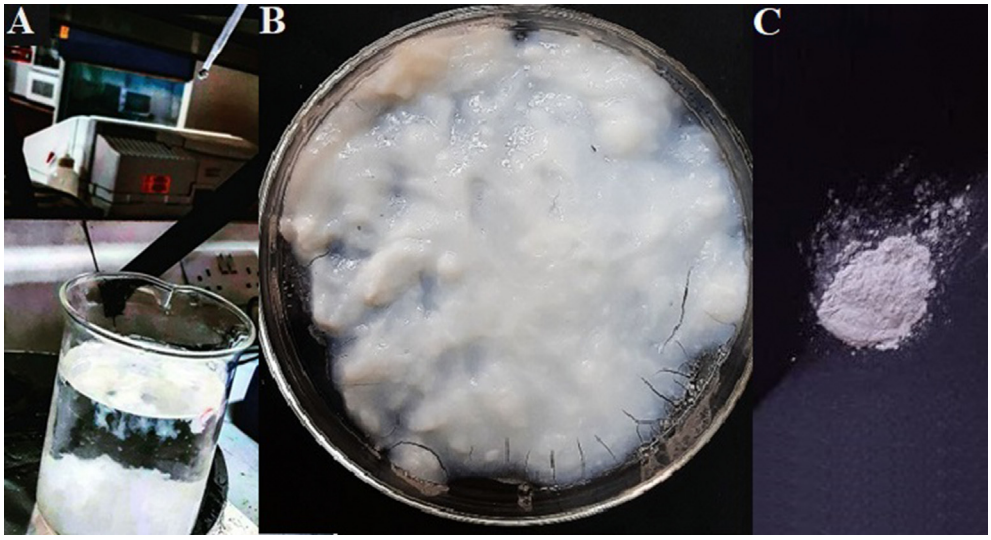

Fig. 1. (A) The alkaline solution is applied dropwise to the Zirconium Oxychlorideoctahydrate solution, (B) Zirconium dioxide gel before drying in the oven, (C) ZrO_2-NP after annealing.

We would be able to investigate both chemically direct analytical composition and nanopowder shape using Energy dispersive X-ray (EDX) and SEM [32]. EDX analysis was used to measure the ratio of ZrO_2 in the sample, which was prepared as a thin film for the experiment.

This procedure enabled us to examine the sample's morphology and elemental content. Day Petronic Company, Tehran, Iran, conducted this analysis.

2.4. Preparation of PMMA and PMMA/NPs composite

To standardize acrylic resin specimens, molds were made from a metallic square pattern with suitable measurements for the future specimen (height: 3 mm; diameter: 40 mm). The heat-polymerized denture base poly methyl methacrylate resin (Superacryl Plus powder, SpofaDental a.s., Jicin, Czech Republic) was prepared under the manufacturer's recommendations. 6 g of powder was combined with 2.5 ml of monomer for each specimen, using a previously developed procedure [33]. The powder contains ZrO_2-NPs in various percentages based on polymer mass: 1 wt%, 2 wt%, 3 wt%, and 10 wt%. The exact ratios were generated using TiO_2-NPs and a sample containing 3wt% nanoparticles as a combination of ZrO_2-NPs and TiO_2-NPs. As controls, nano particle-free specimens were prepared.

The nanocomposites were immediately packed into the dental flask molds made of dental stone. Specimens were pressed to 1 ton using a hydraulic press (Manual hydraulic press 10 TON SHOP PRESS) [34], then polymerized the acrylic resin using a standard electric heater by immersing them in room temperature water and raising the water temperature until it boiled within 1 h under the directions provided by the manufacturer for the curing process. The specimens were taken from the flask after cooling [33]. Then, by using three sheets of sandpaper consecutively (500p, 1000p, and 2000p) to minimize the surface roughness [35], all samples were polished and cut into 16 specimens to make the ideal final sample for our procedures (height: 3 mm; diameter: 10 mm), we created ten groups of sixteen samples each, for a total of 160 samples (see Table 1).

2.5. Shore durometer hardness methodology

In recent years, the medical industry has seen a rise in the use of metallic implants designed to

Table 1. The PMMA samples reinforced by different ratios of NPs.

Samples	ZrO_2-NPs wt%	TiO_2-NPs wt%	PMMA wt%
Pure PMMA	0	0	100
TiO_2-1	0	1	99
TiO_2-2	0	2	98
TiO_2-3	0	3	97
TiO_2-10	0	10	90
3 TZ-3	1.5	1.5	97
ZrO_2-1	1	0	99
ZrO_2-2	2	0	98
ZrO_2-3	3	0	97
ZrO_2-10	10	0	90

endure high levels of mechanical stress [36]. Hardness testing is a typical material property test. Depending on the hardness specimens test type, hardness testing analyzes materials' indent penetration or other surface properties [37].

The Shore Durometer (D) scale was used to measure the hardness of acrylic resin samples. Rigid polymers, hard rubber, and semi-rigid plastics are tested on the Shore D scale. Using a durometer D-XD, a total of five points in each sample were analyzed to arrive at the findings. The test was conducted at the University of Technology – Baghdad in Iraq (Shore hardness tester TH210).

2.6. The apparent porosity

Porosity directly impacts microbe adhesion in PMMA; hence, increasing the apparent porosity will improve adhesion.

We examined the apparent porosity using Archimedes' principle. This method is based on the weight change of samples when wet and dry, as well as the weight of samples while immersed in water [38]. The following equation was used to calculate the samples' apparent porosity [39]:

$$\text{The apparent porosity} = (S - D)/(S - I) \times 100\% \quad (1)$$

D: Weight of the dray sample.
S: Weight of the saturating sample.
I: Weight of the immersed sample.

2.7. Blood compatibility

2.7.1. Hemolysis assay

The specimens are first sterilized and then immersed in 2 ml of 0.9 sodium chloride for 2 days at 25 °C. A healthy volunteer gave blood, centrifuged to separate the red blood cells (RBC) from the plasma, and then washed five times to remove any leftover plasma from the RBC. Then, 1 ml of RBC was mixed with 4 ml of phosphate-buffered saline (PBS) to create a 20% v/v RBC suspension. 0.5 ml of the sample solution was transferred to a 200 μl suspension and maintained in a water bath for 90 min at 37 °C. The suspension was centrifuged for 4 min at 1000 RPM, and the optical density of the filtrate solution at 541 nm was determined using a spectrophotometer.

The positive control consisted of 200 μl of RBC suspension in 1 ml of water, while the negative control consisted of 200 μl of RBC suspension in 1 ml of PBS. Three tests were done concurrently on each sample group. The hemolysis ratio was calculated using the following equation:

$$\text{Hemolysis}\% = (\text{As} - \text{An})/(\text{Ap} - \text{An}) \times 100\% \quad (2)$$

The absorbance of the sample, negative, and positive control, respectively, are denoted by As, An, and Ap.

For the blood film formation, the sediment (RBCs) was stained for 2 min with Leishman stain, dried, and rinsed with distilled water. A 40× magnification light microscope was used to examine the blood film [40].

2.7.2. Prothrombin time (PT) and the international normalized ratio (INR) assay

For 48 h, samples of PMMA composite were immersed in 0.5 ml of 0.9% sodium chloride. After drawing blood from a healthy volunteer, the blood was put in tubes with sodium citrate, centrifuged, and 180 μl of plasma was mixed with 20 μl of the sample solution. Then, 50 μl of this combination was added to semi-automated equipment (from Human Company, Germany) and incubated at 37 C°, followed by the addition of 100 μl of thromboplastin liquid and the recording of Prothrombin time (PT) and international normalized ratio (INR) values.

0.9 sodium chloride was employed as a control. Each sample group was analyzed three times in a row [41].

2.8. Bacterial adhesion and colonization

There are numbers of oral conditions that may lead to more serious health difficulties if microorganisms adhere to particular mouth surfaces and dental plaque forms on these areas; *S. aureus,* a Gram-positive bacteria, and *Klebsiella pneumoniae (K. pneumoniae),* a Gram-negative bacteria, were obtained from Yarmouk Teaching Hospital patients, cultured on MacConkey agar, isolated, stained with Gram stain, and identified using VITEK® 2.

To begin the experiment, stock solutions of bacteria containing 1.48108 cells/ml were produced in normal saline. The autoclave was used to sanitize all of the samples for 15 min 10 μl of the stock was applied to the surface of each sample under sterilizing conditions and incubated for 4 h.

Three washing with 0.9 percent sodium chloride were performed to remove the unattached or inhibited bacteria from the sample's surface. After centrifugation for 20 min at 4000 RPM with 1 ml of 0.9 percent sodium chloride, unattached and inhibited bacteria were released from the specimen surface into the solution using a previously developed procedure [42]. Following that, using the spread plate technique, 50 μl of the solution was

grown on MacConkey Agar for *K. pneumoniae* and nutrient agar for *S. aureus*. As a control, we used a sample made entirely of PMMA.

2.9. Statistical analysis

By comparing the means of three groups, the significance of variances across groups and the standard error of the mean (SE) were investigated by using the one-way analysis of variance (ANOVA) was used, followed by a posthoc Tukey test to validate the statistical difference between the means and compare them to the means of the control sample. The following are the significance values for a one-way analysis of variance (ANOVA): (not significant: $p > 0.05$, $*p < 0.05$, $**p < 0.01$, and $***p < 0.001$).

OriginPro 2021b (OriginLab, Northampton, MA, USA) and GraphPad Prism 9.3.0 were used to calculate statistical significance (Software, Inc., San Diego, CA, USA). OriginPro 2021b was used to fit the values to the plotted points.

3. Results and discussion

3.1. ZrO_2 nanoparticles characterization

3.1.1. X- Ray Diffraction technique (XRD)

Figure 2 shows the XRD pattern of the generated ZrO_2 nanoparticles, which is similar to the XRD pattern peaks of amorphous ZrO_2 in *(C.O. Chikere* et al.*)* study [43], which displayed similar characteristic peaks of 2 theta degree (8.4º, 31.3º, and 53º). On examination of the structures, one can see the large peak of tetragonal ZrO_2 and another of monoclinic ZrO_2. For example, the presence of [Zr $(OH)_4$+2.H_2O]4 + 2(OH)8 hydroxo-complex during the generation stage may explain the formation of tetragonal-shaped zirconia, the main phase of nanoparticles. The hydroxide complex has previously been linked to zirconia nanoparticle synthesis. This work attributed the predominant tetragonal phase to the presence of NaOH throughout the hydroxo–formation complex's stage [43,44] (see Table 2).

3.1.2. Energy dispersive X-ray spectroscopy (EDX)

While the EDX spectrum of pure ZrO_2 has peaks for the elements Zr and O, the EDX spectrum of composites includes peaks for the elements Oxygen (O), Carbon (C), chlorine (Cl), Hafnium (Hf), and zirconium (Zr). Due to small peaks of C, Cl, and Hf in the spectrum, negligible contaminants have been discovered. The intensities of the O and Zr peaks vary linearly with the concentrations of their respective predecessors of ZrO_2, around 74:15 is the Zr/O weight ratio, as seen in Fig. 3.

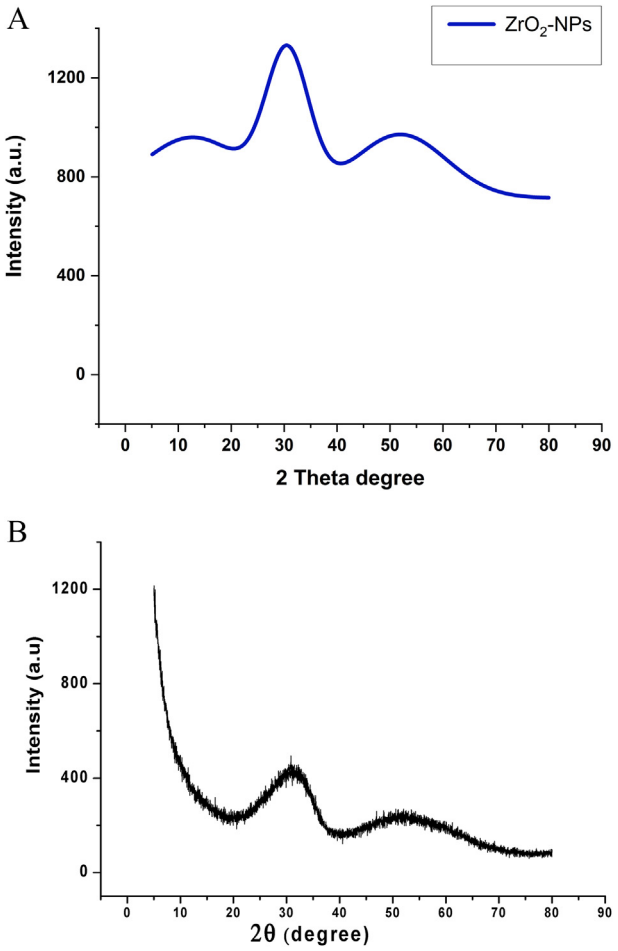

Fig. 2. (A) The XRD of the ZrO_2-NPs sample generated in this research reveals that the peaks are identical to those of a ZrO_2-NPs sample from a prior work in shape (B) [43].

3.1.3. Scanning electron microscope (SEM)

The shape and microstructure of the sample were investigated using the scanning electron microscope (SEM), as shown in Fig. 4. The particles in this zirconia sample range from approximately 6 to 18 nm. Figure 5 depicts the Zirconia particle size distribution as seen using a scanning electron microscope (SEM). As previously stated, the average diameter of zirconia particles is 12.63151 nm, which will fill up the pores in the resin samples.

Table 2. Peak list.

Pos. [°2Th.]	Height [cts]	FWHMLeft [°2Th.]	d-spacing [Å]	Rel. Int. [%]
8.4 (4)	131 (97)	2 (1)	10.49451	45.91
31.3 (4)	285 (51)	9 (1)	2.85971	100.00
53 (1)	100 (42)	10 (2)	1.71912	35.07

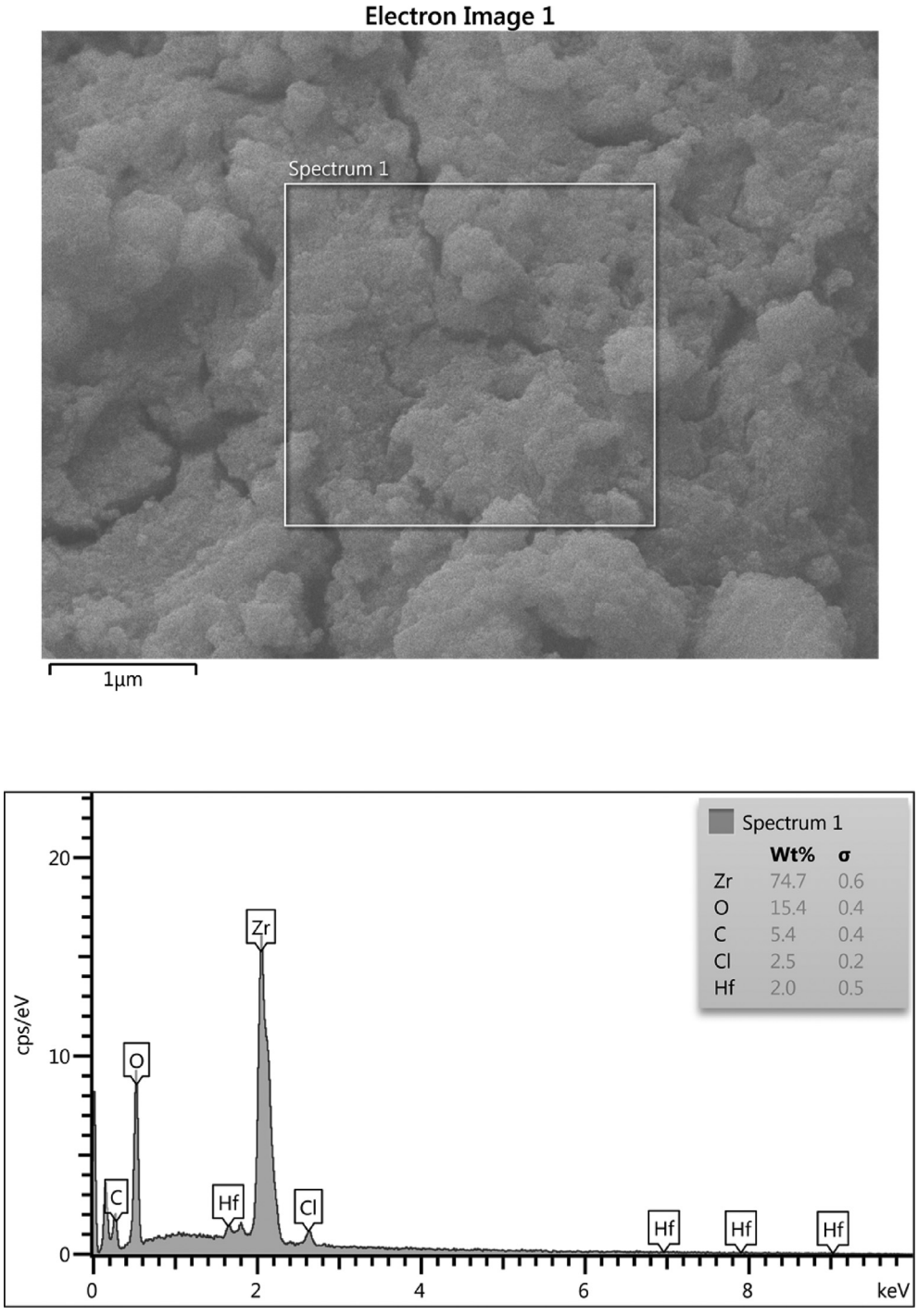

Fig. 3. The SEM images and EDX spectrum of zirconia powder.

3.2. Hardness shore D

Figure 6 depicts a histogram of the hardness values of PMMA and its composites. ZrO_2 and TiO_2 nanoparticles distributed in PMMA-NPs composites considerably increase the hardness qualities compared to pure PMMA.

Additionally, TiO_2-NPs have a better potential to increase the hardness of the resin alloy than ZrO_2-NPs. However, the hardness properties of ZrO2-NPs in ZrO2-NPs-rich acrylic resin samples are significant compared to pure acrylic resin. Since specimens' hardness ratios grow linearly with increasing hardness, a specimen containing 10 wt%

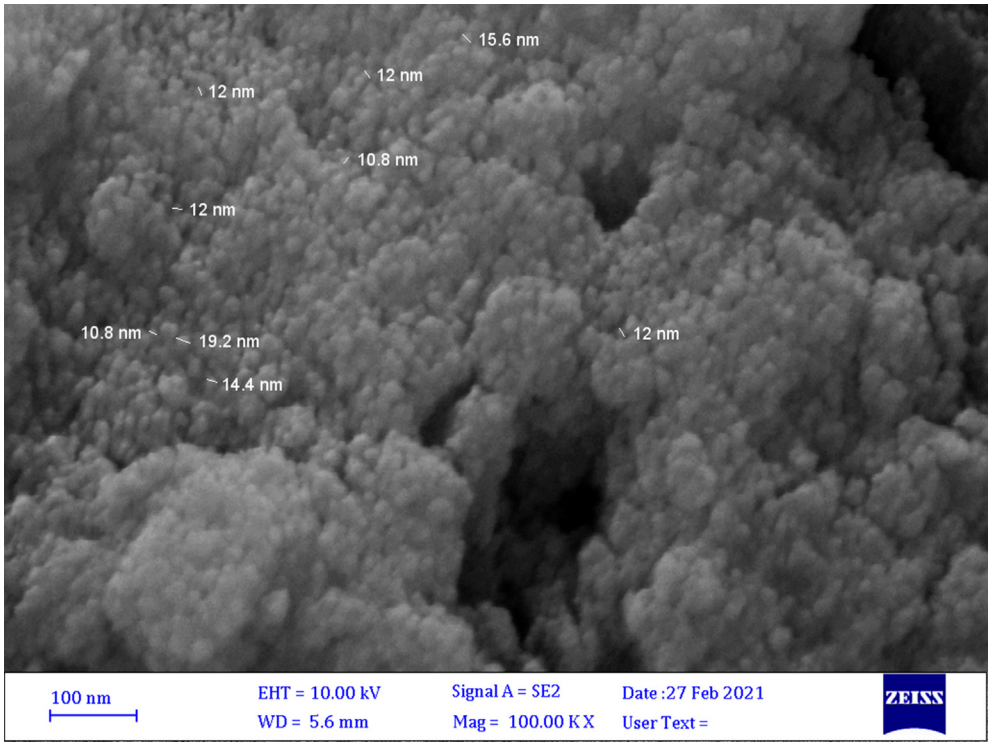

Fig. 4. Zirconia imaged using scanning electron microscopy (SEM).

TiO_2-NPs surpassed all others (91.0 N/mm^2) in terms of hardness; furthermore, due to the synergistic interaction between ZrO_2 and TiO_2, 3 wt% ZrO_2–TiO_2 exhibited superior results in hardness than 3 wt% ZrO_2 or 3 wt% TiO_2 alone. Its results are comparable to those of other researchers *(Mina S.* et al.*)* [45].

3.3. The apparent porosity ratio

Reducing surface roughness and apparent porosity on the specimens' surfaces are important factors restricting bacterial adhesion. As shown in this study (Fig. 7), apparent porosity is consistently reduced when nanoparticles are continually incorporated into PMMA; the specimens containing 10 wt% of the total weight of nanoparticles had the lowest percentage of porosity. Due to the synergistic interaction between ZrO_2 and TiO_2 [45], 3 wt% ZrO_2–TiO_2 displayed a lower apparent porosity value than 3 wt% ZrO_2 or 3 wt% TiO_2 alone.

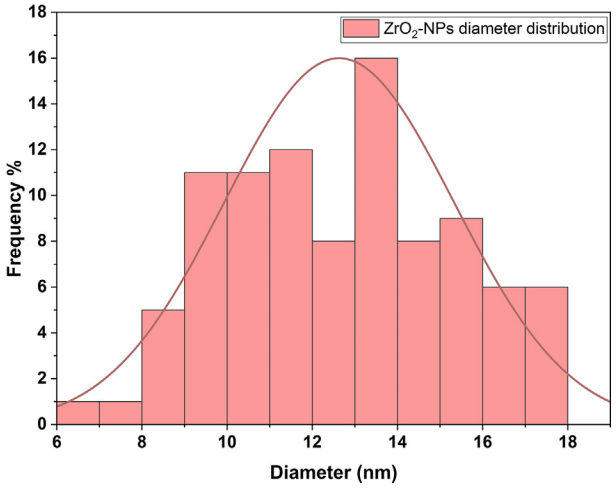

Fig. 5. The size distribution of zirconium dioxide nanoparticles.

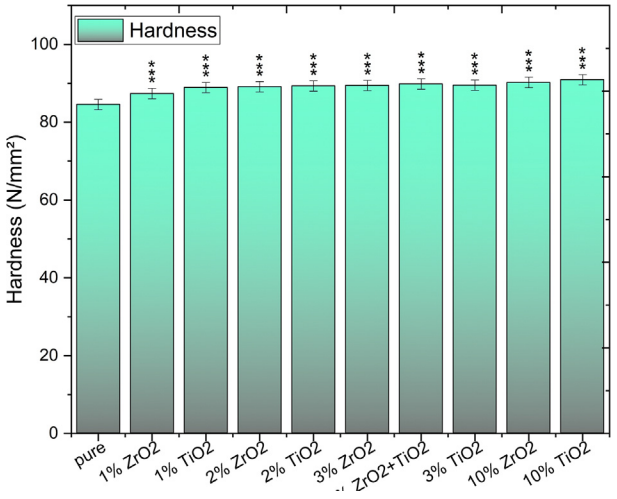

*Fig. 6. Significant increase in hardness values in all composites materials. ***P < 0.001.*

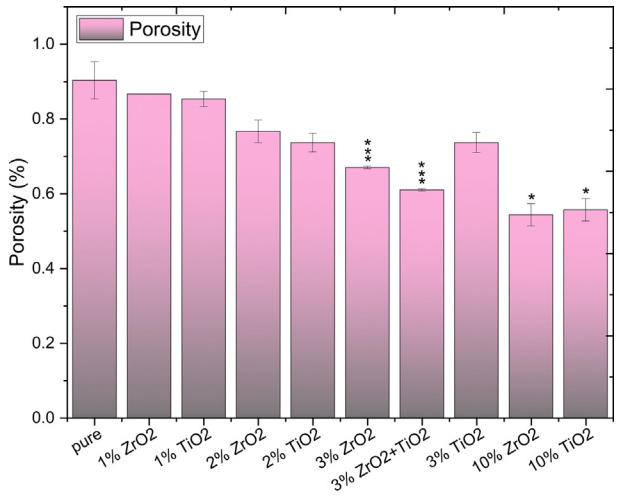

*Fig. 7. This graph represents the decrease in apparent porosity of nano-oxides composite samples as compared to pure samples. *P < 0.05, ***P < 0.001.*

3.4. Blood compatibility assays (in-vitro)

3.4.1. Hemolysis assay

This project aimed to develop clinically viable PMMA composite resins that would directly contact human tissue and blood. When composite materials fail to meet the blood compatibility performance standards, it not only affects their clinical application in the oral region but also poses severe health risks to the rest of the body.

In this study, we have tested the blood compatibility of PMMA resin composite samples using hemolysis, INR, and PT. Compared to a positive control that completely hemolyzed RBCs, the lower concentration ranges of PMMA-NPs composites exhibited no adverse impact on RBC shape. Most hemolysis occurred in a composite sample containing 10 wt. % ZrO2-NPs remained within the normal range (0–5%).

According to this research, nanoparticle composites might be employed in several applications since they are particularly compatible with blood if used in low quantities (Fig. 8).

3.4.2. Prothrombin time (PT) and the international normalized ratio (INR) assay

In the case of TiO_2-NPs-PMMA composites, all samples have a statistically significant influence on PT and INR values, and it is not suggested to use any of them, despite the effect of 1 wt% TiO_2-NPs. Even though the TiO_2-NPs sample is still within the normal range (12–15), employing a combination of TiO_2-NPs and ZrO_2-NPs has shown better biocompatibility results than using TiO_2-NPs alone.

On the other site, ZrO_2-NPs had a lower influence on PT & INR values than TiO_2-NPs. They so could be suggested for denture base manufacture and further use, with the exception of a high ratio of ZrO_2-NPs (10 wt%), which had a considerable effect on PT & INR values, preventing its usage at high ratios (Fig. 8).

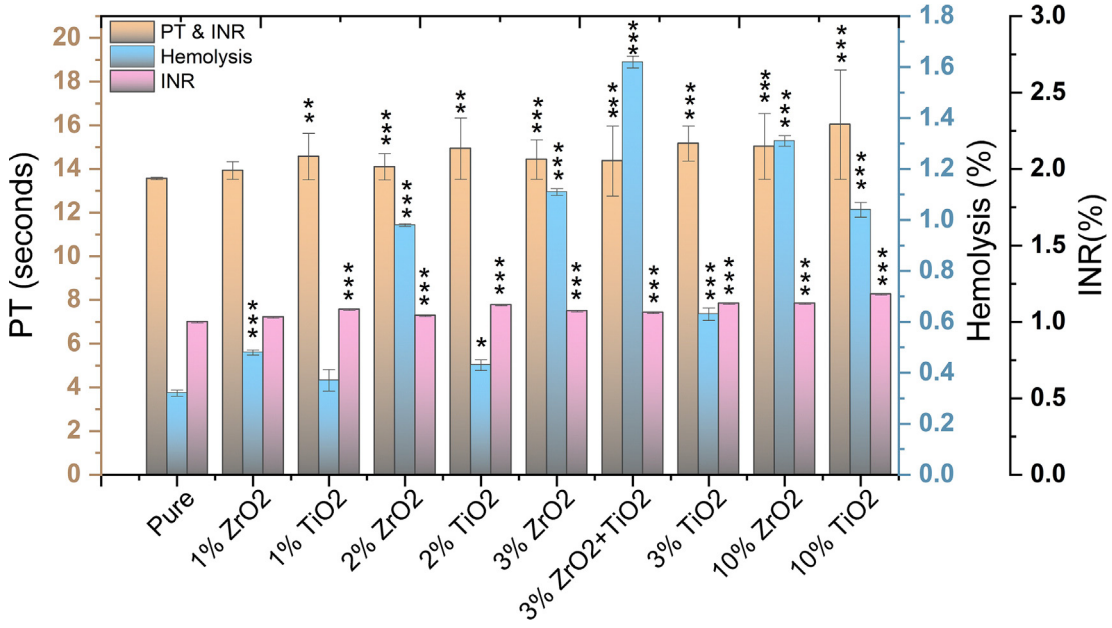

*Fig. 8. This chart shows the biocompatibility (hemolysis, PT, and INR) of nano-oxide composite materials compared to the pure samples. *P < 0.05, **P < 0.01, ***P < 0.001.*

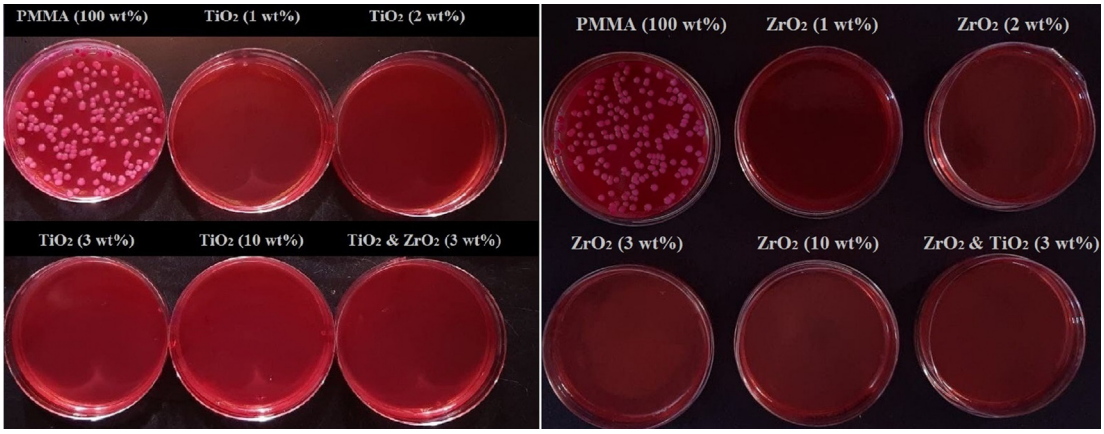

Fig. 9. As seen in this figure, nano-oxide composites have a considerable effect on K. pneumoniae that have been cultured on MacConkey agar plates.

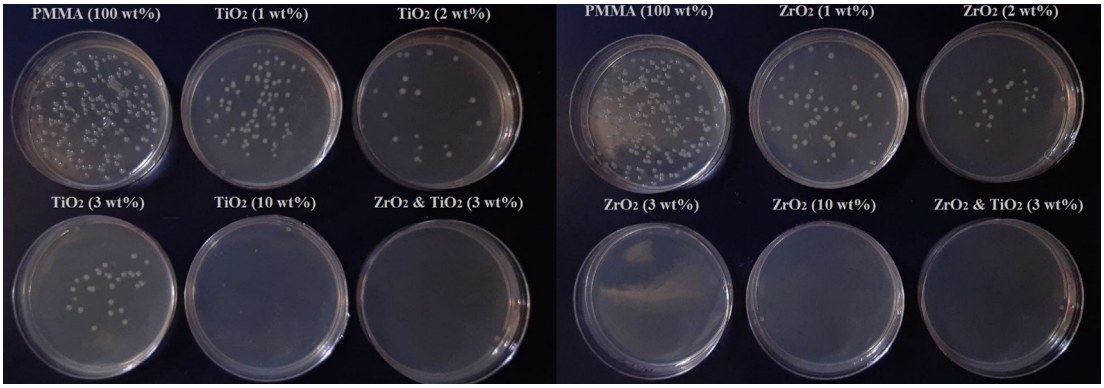

Fig. 10. This figure shows the colony forming units (CFU) of S. aureus bacteria on nutrient agar plates cultured using the spread plate technique.

3.6. Inhibition of the bacterial adhesion and colonization to PMMA-NPs composites

We remarked from the results of this study that all nano-oxides composite samples have the potential to minimize adhesion and inhibit the growth of *K. pneumoniae* on the samples' surfaces, unlike with pure samples, where we can clearly identify and count *K. pneumoniae* colonization on the surface of the sample on MacConkey agar, as seen in Fig. 9. In terms of *S. aureus* bacteria, we discovered that the reinforced samples with (3 wt% and 10 wt% ZrO_2 NPs, 10 wt% TiO_2 NPs, and 3 wt% ZrO_2–TiO_2 NPs) had more effectiveness than the other samples with lower percentages of nano-oxides, and we observe more intense growth in the pure samples, Fig. 10.

These findings can be explained by a decrease in the porosity of the sample surfaces, which reduced bacterial adhesion, as well as the ROS (O_2, OH, H_2O_2, and HO_2) produced by nano-oxide particles, which have the ability to inhibit bacterial growth by interacting with cell membranes, DNA, and thiol groups in proteins to have antimicrobial effects, these findings are comparable to those of *(Guofeng S.* et al.*)* [46] who confirmed the antibacterial action of nano-oxide materials.

The significant inhibition of *S. aureus* growth on the surface of the 3 wt% ZrO_2–TiO_2 NPs composite samples and the presence of *S. aureus* on the surface of the 3 wt% TiO_2 NPs composite samples was a consequence of the synergistic interaction between ZrO_2 and TiO_2, comparable to the findings of *(Yinghan* L. et al.*)* [47].

4. Conclusion

The magnitude of the measured values suggests that the 3 wt% PMMA-ZrO_2 and 3 wt% PMMA-ZrO_2-TiO_2 composites showed the best results in terms of their inhibition of bacterial growth and their effects on biocompatibility (hemolysis, PT, and INR) within the normal limit, unlike previous composite samples with higher nano-oxide ratios that exhibit stronger antibacterial efficacy but also a higher influence on biocompatibility in human blood (slightly above the normal range of PT and INR tests).

The findings also revealed a significant rise in hardness values and a significant reduction in porosity values when the weight ratios of the nano-oxides increased in all samples.

5. Recommendations

The author recommends further study of the samples in this study on animal blood and tissue.

Conflict of interests

There is no conflict of interest

Acknowledgments

I thank Allah for bestowing my health and strength and driving me to do this study, as well as for my parents, siblings, friends, and the whole staff of the DNA and Sihati Al-jamiaa laboratories.

References

[1] S.A. Ibrahim, S.H. Lafta, W.A. Hussain, Impact strength of surface treated SS316L wires reinforced PMMA. 30 (2021) 272–278.

[2] S.Y. Taher, W.A. Hussain, The effect of acidic treatment of carbon fiber on denture mechanical properties, J Phys Conf Ser. 1879 (2021) 1–10, https://doi.org/10.1088/1742-6596/1879/3/032082.

[3] W.A. Hussain, S.M.H. Al-Jawad, S.A. Hannon, Effect of carbon fibre layer with alumina and tri calcium phosphate on mechanical properties of denture base, Int J Nano Biomaterials (IJNBM). 10 (2021) 22–33, https://doi.org/10.1504/IJNBM.2021.114691.

[4] Z.S.A. Karkosh, B.M.A. Hussein, W.M.A. Alwattar, Effect of phosphoric containing and varnish-coated groups on candida albicans adhesion and porosity of heat cure acrylic denture base material, Biomed Pharmacol J. 11 (2018) 179–185, https://doi.org/10.13005/bpj/1360.

[5] L. Costa de Medeiros Dantas, J. Paulo da Silva-Neto, T. Souza Dantas, L. Zago Naves, F. Domingues das Neves, A. Soares da Mota, Bacterial adhesion and surface roughness for different clinical techniques for acrylic polymethyl methacrylate, Int J Dent. 2016 (2016) 1–6.

[6] E. Günther, N. Kommerein, S. Hahnel, Biofilms on polymeric materials for the fabrication of removable dentures, "Greetings Day! "Unsolicited e-Mails from Quest, Op J. 2 (2020) 142–151.

[7] W.J. Loesche, Microbiology of dental decay and periodontal disease, University of Texas Medical Branch at Galveston. (1996). https://www.ncbi.nlm.nih.gov/books/NBK8259/. (accessed December 26, 2021).

[8] B. Corrin, A.G. Nicholson, Development of the lungs; perinatal and developmental lung disease, in: A.G.N. Bryan Corrin, eds., Pathol. Lungs, Churchill Livingstone, 2011: pp. 39–90, https://doi.org/10.1016/b978-0-7020-3369-8.00002-1.

[9] S. Modi, R. Prajapati, G.K. Inwati, N. Deepa, V. Tirth, V.K. Yadav, K.K. Yadav, S. Islam, P. Gupta, D.H. Kim, B.H. Jeon, Recent trends in fascinating applications of nanotechnology in allied health sciences, Crystals. 12 (2022) 1–16, https://doi.org/10.3390/cryst12010039.

[10] C.N. Fries, E.J. Curvino, J.L. Chen, S.R. Permar, G.G. Fouda, J.H. Collier, Advances in nanomaterial vaccine strategies to address infectious diseases impacting global health, Nat Nanotechnol. 16 (2021) 1–14, https://doi.org/10.1038/s41565-020-0739-9.

[11] H. Arshad, M. Saleem, U. Pasha, S. Sadaf, Synthesis of Aloe vera-conjugated silver nanoparticles for use against multi-drug-resistant microorganisms, Electron J Biotechnol. 55 (2022) 55–64, https://doi.org/10.1016/j.ejbt.2021.11.003.

[12] N.J. Hunt, P.A.G. McCourt, Z. Kuncic, D.G. Le Couteur, V.C. Cogger, Opportunities and challenges for nano-therapeutics for the aging population, Front Nanotechnol. 4 (2022) 1–15, https://doi.org/10.3389/fnano.2022.832524.

[13] V. De Matteis, L. Rizzello, Noble metals and soft bio-inspired nanoparticles in retinal diseases treatment: a perspective, Cells. 9 (2020) 1–23, https://doi.org/10.3390/cells9030679.

[14] W. Song, S. Ge, Application of antimicrobial nanoparticles in dentistry, Molecules. 24 (2019) 1–15, https://doi.org/10.3390/molecules24061033.

[15] M.M. Gad, R. Abualsaud, Behavior of PMMA denture base materials containing titanium dioxide nanoparticles: a literature review, Int J Biomater. 2019 (2019) 1–14, https://doi.org/10.1155/2019/6190610.

[16] G. Singh, A. Agarwal, M. Lahori, Effect of cigarette smoke on the surface roughness of two different denture base materials: an in vitro study, J Indian Prosthodont Soc. 19 (2019) 42–48, https://doi.org/10.4103/jips.jips.

[17] N.C. Joshi, N. Chaudhary, N. Rai, Medicinal plant leaves extract based synthesis, characterisations and antimicrobial activities of ZrO2 nanoparticles (ZrO2 NPs), Bionanoscience. 11 (2021) 497–505, https://doi.org/10.1007/s12668-021-00829-2.

[18] S. Gowri, R. Rajiv Gandhi, M. Sundrarajan, Structural, optical, antibacterial and antifungal properties of zirconia nanoparticles by biobased protocol, J Mater Sci Technol. 30 (2014) 782–790, https://doi.org/10.1016/j.jmst.2014.03.002.

[19] A.A. Thamir, N.J. Jubier, J.F. Odah, Antimicrobial activity of zirconium oxide nanoparticles prepared by the sol-gel method, J Phys Conf Ser. 2114 (2021) 1–8, https://doi.org/10.1088/1742-6596/2114/1/012058.

[20] A. Jaafar, C. Hecker, P. Árki, Y. Joseph, Sol-gel derived hydroxyapatite coatings for titanium implants: a review, Bioengineering. 7 (2020) 1–23, https://doi.org/10.3390/bioengineering7040127.

[21] Z. Mohammed, S. Khalil, M. Mutter, Synthesis and characterization of ZrO2: MgO thin films by plasma of R.F. Magnetron sputtering, Karbala Int J Mod Sci. 5 (2019) 12–18, https://doi.org/10.33640/2405-609X.1064.

[22] S.S. Al-Tae'E, O.M. Almitwalli, S.B.H. Farid, Preparation of glass ionomer cement from recycled low alumina glass, Karbala Int J Mod Sci. 6 (2020) 141–147, https://doi.org/10.33640/2405-609X.1410.

[23] S. Priyadarsini, S. Mukherjee, M. Mishra, Nanoparticles used in dentistry: a review, J Oral Biol. Craniofacial Res. 8 (2018) 58–67, https://doi.org/10.1016/j.jobcr.2017.12.004.

[24] M. Ikram, M. Rashid, A. Haider, S. Naz, J. Haider, A. Raza, M.T. Ansar, M.K. Uddin, N.M. Ali, S.S. Ahmed, M. Imran, S. Dilpazir, Q. Khan, M. Maqbool, A review of photocatalytic characterization, and environmental cleaning, of metal oxide nanostructured materials, Sustain Mater Technol. 30 (2021) 343, https://doi.org/10.1016/j.susmat.2021.e00343.

[25] L.A. Pham-Huy, H. He, C. Pham-Huy, Free radicals, antioxidants in disease and health, Int J Biomed Sci. 4 (2008) 89–96, pmc/articles/PMC3614697/(accessed May 23, 2022).

[26] M.Y. Memar, R. Ghotaslou, M. Samiei, K. Adibkia, Antimicrobial use of reactive oxygen therapy: current insights, Infect Drug Resist. 11 (2018) 567–576, https://doi.org/10.2147/IDR.S142397.

[27] A. Ashfaq, M. Ikram, A. Haider, A. Ul-Hamid, I. Shahzadi, J. Haider, Nitrogen and carbon nitride-doped TiO2 for multiple catalysis and its antimicrobial activity, Nanoscale Res Lett. 16 (2021) 1–15, https://doi.org/10.1186/s11671-021-03573-4.

[28] S.A. Naji, T.S.J. Kashi, M. Pourhajibagher, M. Behroozibakhsh, R. Masaeli, A. Bahador, Evaluation of antimicrobial properties of conventional poly(Methyl methacrylate) denture base resin materials containing

hydrothermally synthesised anatase Tio 2 nanotubes against cariogenic bacteria and candida albicans, Iran, J Pharm Res. 17 (2018) 161–172, pmc/articles/PMC6447881/(accessed May 22, 2022).
[29] M. Ikram, R. Asghar, M. Imran, M. Naz, A. Haider, A. Ul-Hamid, J. Haider, A. Shahzadi, W. Nabgan, S. Goumri-Said, M.B. Kanoun, A.Rafiq Butt, Experimental and computational study of Zr and CNC-doped MnO 2 nanorods for photocatalytic and antibacterial activity, ACS Omega. 7 (2022) 14045–14056, https://doi.org/10.1021/acsomega.2c00583.
[30] J. Verran, G. Sandoval, N.S. Allen, M. Edge, J. Stratton, Variables affecting the antibacterial properties of nano and pigmentary titania particles in suspension, Dyes Pigments. 73 (2007) 298–304, https://doi.org/10.1016/j.dyepig.2006.01.003.
[31] M.R.H. Siddiqui, A.I. Al-Wassil, A.M. Al-Otaibi, R.M. Mahfouz, Effects of precursor on the morphology and size of ZrO2 nanoparticles, synthesized by sol-gel method in non-aqueous medium, Mater Res. 15 (2012) 986–989, https://doi.org/10.1590/S1516-14392012005000128.
[32] S. Tinkov, Contemporary industrial practice for manufacturing of nanomedicines, in: Emerg. Appl. Nanoparticles Archit. Nanostructures Curr. Prospect. Futur. Trends, Elsevier Inc., 2018: pp. 447–500, https://doi.org/10.1016/B978-0-323-51254-1.00015-4.
[33] Z. Hasratiningsih, V. Takarini, A. Cahyanto, Y. Faza1, L.A.T.W. Asri, B.S. Purwasasmita, Hardness evaluation of PMMA reinforced with two different calcinations temperatures of ZrO2-Al2O3-SiO2 filler system, J Phys Conf Ser. 755 (2016) 1–17, https://doi.org/10.1088/1742-6596/755/1/011001.
[34] D.R. Monteiro, L.F. Gorup, A.S. Takamiya, E.R. de Camargo, A.C.R. Filho, D.B. Barbosa, Silver distribution and release from an antimicrobial denture base resin containing silver colloidal nanoparticles, J Prosthodont. 21 (2012) 7–15, https://doi.org/10.1111/j.1532-849X.2011.00772.x.
[35] I. De-la-Pinta, M. Cobos, J. Ibarretxe, E. Montoya, E. Eraso, T. Guraya, G. Quindós, Effect of biomaterials hydrophobicity and roughness on biofilm development, J Mater Sci Mater Med. 30 (2019) 1–11, https://doi.org/10.1007/s10856-019-6281-3.
[36] M.T. Mohammed, S.M. Hussein, Evaluation of structure and properties of various sol-gel nanocoatings on biomedical titanium surface, Karbala Int J Mod Sci. 6 (2020) 215–224, https://doi.org/10.33640/2405-609X.1630.
[37] H.K. Hameed, H.A. Rahman, The effect of addition nano particle ZrO2 on some properties of autoclave processed heat cure acrylic denture base material, J Baghdad Coll Dent. 27 (2015) 32–39, https://doi.org/10.12816/0015262.
[38] W.A. Hussain, E.M. Hadi, M.M. Ismail, L.H. Alwan, Preparation of household water filter, J Appl Sci Eng. 23 (2020) 61–68, https://doi.org/10.6180/jase.202003_23(1).0008.
[39] A.A. Jock, F.A. Ayeni, A.S. Ahmed, U.A. Sullayman, Evaluation of the refractory properties of Nigerian ozanagogo clay deposit, J Miner Mater Char Eng. 1 (2013) 321–325, https://doi.org/10.4236/jmmce.2013.16048.
[40] S.H. Ali, G.M. Sulaiman, M.M.F. Al-Halbosiy, M.S. Jabir, A.H. Hameed, Fabrication of hesperidin nanoparticles loaded by poly lactic co-Glycolic acid for improved therapeutic efficiency and cytotoxicity, Artif. Cells, Nanomedicine Biotechnol. 47 (2019) 378–394, https://doi.org/10.1080/21691401.2018.1559175.
[41] S. Chen, J. Yang, Y. Jia, B. Lu, TiO 2 and PEEK reinforced 3D printing PMMA composite resin for dental denture base applications, Nanomaterials. 9 (2019) 1–18.
[42] K.Y. Nam, Characterization and bacterial anti-adherent effect on modified PMMA denture acrylic resin containing platinum nanoparticles, J Adv Prosthodont. 6 (2014) 207–214, https://doi.org/10.4047/JAP.2014.6.3.207.
[43] C.O. Chikere, N.H. Faisal, P. Kong-Thoo-Lin, C. Fernandez, Interaction between amorphous zirconia nanoparticles and graphite: electrochemical applications for gallic acid sensing using carbon paste electrodes in wine, Nanomaterials. 10 (2020) 1–25, https://doi.org/10.3390/nano10030537.
[44] J. Gambe, J. Jouin, F. Remondiere, P. Thomas, O. Masson, Solvent effect in the nonaqueous synthesis of ZrO2 nanoparticles under alkaline conditions, J Mater Sci. 55 (2020) 2802–2814, https://doi.org/10.1007/s10853-019-04137-9.
[45] M. Shahmohammadi, B.E. Nagay, V.A.R. Barão, C. Sukotjo, G. Jursich, C.G. Takoudis, Atomic layer deposition of TiO2, ZrO2 and TiO2/ZrO2 mixed oxide nanofilms on PMMA for enhanced biomaterial functionalization, Appl Surf Sci. 578 (2022), 151891, https://doi.org/10.1016/j.apsusc.2021.151891.
[46] G. Su, X. Zhong, S. Qiu, J. Fan, H. Zhou, X. Zhou, Preparation of mesoporous silica-based nanocomposites with synergistically antibacterial performance from nano-metal (oxide) and polydopamine, Nanotechnology. 33 (2022), 155702, https://doi.org/10.1088/1361-6528/ac467a.
[47] Y. Liu, S. Wang, Z. Wang, N. Ye, H. Fang, D. Wang, Tio 2, sio 2 and zro2 nanoparticles synergistically provoke cellular oxidative damage in freshwater microalgae, Nanomaterials. 8 (2018) 95, https://doi.org/10.3390/nano8020095.